© 2017. Published by The Company of Biologists Ltd | Development (2017) 144, 452-463 doi:10.1242/dev.144410

RESEARCH ARTICLE

A MAPK cascade couples maternal mRNA translation and degradation to meiotic cell cycle progression in mouse oocytes

Qian-Qian Sha[1,*], Xing-Xing Dai[1,*], Yujiao Dang[2,*], Fuchou Tang[2], Junping Liu[3], Yin-Li Zhang[1,4,‡] and Heng-Yu Fan[1,‡]

ABSTRACT

Mammalian oocyte maturation depends on the translational activation of stored maternal mRNAs upon meiotic resumption. Cytoplasmic polyadenylation element binding protein 1 (CPEB1) is a key oocyte factor that regulates maternal mRNA translation. However, the signal that triggers CPEB1 activation at the onset of mammalian oocyte maturation is not known. We provide evidence that a mitogen-activated protein kinase (MAPK) cascade couples maternal mRNA translation to meiotic cell cycle progression in mouse oocytes by triggering CPEB1 phosphorylation and degradation. Mutations of the phosphorylation sites or ubiquitin E3 ligase binding sites in CPEB1 have a dominant-negative effect in oocytes, and mimic the phenotype of ERK1/2 knockout, by impairing spindle assembly and mRNA translation. Overexpression of the CPEB1 downstream translation activator DAZL in ERK1/2-deficient oocytes partially rescued the meiotic defects, indicating that ERK1/2 is essential for spindle assembly, metaphase II arrest and maternal-zygotic transition (MZT) primarily by triggering the translation of key maternal mRNAs. Taken together, ERK1/2-mediated CPEB1 phosphorylation/degradation is a major mechanism of maternal mRNA translational activation, and is crucial for mouse oocyte maturation and MZT.

KEY WORDS: MAPK cascade, Oocyte maturation, Maternal-zygotic transition, mRNA translation, Female fertility, Meiosis

INTRODUCTION

In vertebrates, fully-grown oocytes are arrested at the diplotene stage of meiosis I, and contain a large amount of maternal mRNAs that are translationally dormant (Chen et al., 2011). Upon meiotic maturation, oocytes undergo two consecutive M phases and arrest again at metaphase of meiosis II (MII). Many maternal mRNAs are translationally activated during this process (Chen et al., 2013; Piccioni et al., 2005). These temporally translated proteins play key roles in meiotic spindle assembly, MII arrest maintenance and mRNA clearance during maternal-zygotic transition (MZT).

The mechanisms of temporal and selective activation of maternal mRNAs are complicated and diverse among species (Komrskova et al., 2014). Cytoplasmic polyadenylation of the 3′-untranslated region (3′-UTR) is largely correlated with mRNA stability and translational activation of mRNA, and plays an essential role in oocyte maturation. Cytoplasmic polyadenylation of maternal mRNAs requires a cytoplasmic polyadenylation element (CPE) that binds specific *trans*-acting proteins (Pique et al., 2008). Studies in *Xenopus* and mouse oocytes found that the CPE-binding protein 1 (CPEB1) mediates cytoplasmic polyadenylation of many CPE-containing mRNAs (Ivshina et al., 2014). During *Xenopus* oocyte maturation, phosphorylation of CPEB on several serine/threonine residues is required for early activation of a class of maternal mRNAs, while a large fraction (70-90%) of CPEB1 proteins undergo a polyubiquitylation-dependent degradation in meiosis I (Mendez et al., 2002; Setoyama et al., 2007). This degradation causes a change in the CPEB/CPE ratio and results in activation of another class of mRNAs. However, the precise mechanism of CPEB1 activation and degradation in mammalian species is not known.

Recently, we reported that meiotic cell cycle-coupled CPEB1 activation in mouse oocyte is essential for translation of maternal mRNAs encoding B-cell translocation gene 4 (*Btg4*), a MZT licensing factor (Yu et al., 2016b). Our studies also found that extracellular signal-regulated kinases 1 and 2 (ERK1/2), two of the best-studied mitogen-activated protein kinase (MAPK) family members, are indispensable for BTG4 protein accumulation after meiotic resumption (Yu et al., 2016b). However, it remains unclear whether ERK1/2 is also required for translational activation of other important maternal mRNAs, and whether ERK1/2 accomplishes this function by regulating CPEB1 phosphorylation and degradation.

The ERK1/2 cascade plays pivotal roles in regulating oocyte meiotic cell cycle progression, but the identity of the phosphorylation substrates of ERK1/2 in mammalian oocytes remain elusive. ERK1/2 inhibition or knockout in mouse oocytes severely impairs microtubule organization and meiotic spindle assembly (Fan and Sun, 2004; Zhang et al., 2015). Deletion of ERK1/2 or their upstream kinase MOS (c-mos Moloney murine sarcoma viral oncogene homolog) leads to precocious sister chromatid separation and oocyte parthenogenetic activation (Verlhac et al., 1996; Zhang et al., 2015). Efforts have been made to identify the ERK1/2 phosphorylation substrates in regulating these processes. Verlhac and colleagues have reported MISS (MAPK interacting and spindle stabilizing) and DOC1R (deleted in oral cancer 1 related) as ERK1/2 substrates that regulate microtubule organization of mouse MII oocytes (Lefebvre et al., 2002; Terret et al., 2003). However, considering the profound influence of ERK1/2 knockout on oocyte meiotic division, the physiological function of MAPK cascade in oocytes could not be sufficiently explained by these mechanisms.

In this study, we provide evidence that ERK1/2 triggers the phosphorylation and degradation of CPEB1 at an early stage of oocyte

[1]Life Sciences Institute, Zhejiang University, Hangzhou 310058, China. [2]Biodynamic Optical Imaging Center, College of Life Sciences, Peking University, Beijing 100871, China. [3]Institute of Aging Research, Hangzhou Normal University, Hangzhou 311121, China. [4]Assisted Reproduction Unit, Department of Obstetrics and Gynecology, Sir Run Run Shaw Hospital, School of Medicine, Zhejiang University, Hangzhou 310016, China.
*These authors contributed equally to this work

‡Authors for correspondence (hyfan@zju.edu.cn; 21118326@zju.edu.cn)

H.-Y.F., 0000-0003-4544-4724

Received 10 September 2016; Accepted 7 December 2016

Development (2017) 144, 452-463 doi:10.1242/dev.144410

meiotic resumption. By activating CPEB1, ERK1/2 couples the translation of a series of maternal mRNAs, including *Dazl*, *Tpx2* and *Btg4*, to meiotic maturation. The translation products of these maternal mRNAs are required for meiotic divisions and MZT. CPEB1 mutants that fail to be phosphorylated and degraded in response to ERK1/2 signaling have dominant-negative effects, and cause oocyte maturation defects similar to ERK1/2 inhibition. The meiosis defects caused by ERK1/2 deficiency were partially rescued by exogenous expression of *Dazl*, a CPEB1 downstream mRNA translation activator. Taken together, we elucidated the fundamental role of ERK1/2 in regulating oocyte meiotic maturation and MZT: ERK1/2 trigger meiosis-dependent maternal mRNA translation by activating CPEB1.

RESULTS

ERK1/2 promotes *Btg4* mRNA translation as a ubiquitous regulation mechanism in mammals

We recently reported that ERK1/2 activity is required to activate translation of *Btg4*mRNA, by targeting the three CPEs in its 3′-UTR (Yu et al., 2016b). This important mechanism couples maternal mRNA decay to mouse oocyte maturation. Therefore, we investigated whether it is conserved in other mammals such as pigs. In isolated pig oocytes, BTG4 protein was undetectable in germinal vesicle (GV) oocytes, but was highly expressed after germinal vesicle breakdown (GVBD), indicating that its expression was also coupled with oocyte maturation (Fig. 1A). The MEK1/2 inhibitor U0126 blocked ERK1/2 activation as well as BTG4 accumulation (Fig. 1B). CNOT7, the BTG4-targeted RNA deadenylase, showed a similar meiotic maturation-coupled and ERK1/2-dependent expression pattern to BTG4 (Fig. 1A,B). The crucial CPE sites in the 3′-UTR of mouse *Btg4* were conserved in pigs (Fig. 1C). Similar to our observations in mouse, the 3′-UTR of pig *Btg4* was activated only after meiotic resumption, and in an ERK1/2-dependent manner (Fig. 1D), suggesting that this is a ubiquitous regulation mechanism in mammals.

ERK1/2 deletion in mouse oocyte causes female infertility associated with maternal-zygotic transition defects

To investigate whether maternal ERK1/2 in mouse oocytes is required for MZT, we selectively deleted *Erk2* in oocytes with an *Erk1*$^{-/-}$ background using transgenic mice expressing *Gdf9* promoter-mediated *Cre* recombinase (*Erk1*$^{-/-}$;*Erk2*$^{fl/fl}$;*Gdf9-Cre*, later referred to *Erk1/2*$^{oo-/-}$). Efficient ERK1/2 deletion was confirmed by western blotting using isolated oocytes from wild-type and *Erk1/2*$^{oo-/-}$ females, and oocyte-specific ERK1 deletion was also demonstrated using immunohistochemistry (Fig. 2A,B). The *Erk1/2*$^{oo-/-}$ females were sterile, whereas the males exhibited normal fertility. *Erk1/2*-deleted oocytes resume meiotic maturation (characterized by GVBD) at a similar rate to wild-type oocytes (Fig. 2C). However, the polar body 1 (PB1) emission was delayed after ERK1/2 deletion (Fig. 2D). Spindles with distorted shapes were observed in these oocytes (Fig. 2E). We then determined whether ERK1/2 was also required for MZT. *Erk1/2*$^{oo-/-}$ females were superovulated and then mated with wild-type males. When most control zygotes developed to the 2-cell stage at 1.5 days post-coitus (1.5 dpc), a remarkable proportion of zygotes from *Erk1/2*$^{oo-/-}$ mice were arrested at the zygote stage (76%, *n*=162) and quickly degenerated (Fig. 2F,G). Only 24% (*n*=46) of maternal ERK1/2-deleted embryos developed to the 2-cell stage, and 12% (*n*=56) developed to the 4-cell stage (2.5 dpc), but none developed into blastocysts at 4 dpc (Fig. 2F,G).

Maternal transcript degradation during GV-to-MII transition is blocked in *Erk1/2*$^{oo-/-}$ oocytes

Because ERK1/2 activity is required for accumulation of BTG4 protein and MZT, we compared the global mRNA levels between *Erk1/2*$^{oo-/-}$ and wild-type oocytes at GV and MII stages using RNA-seq analyses. Differential expression of transcripts was analyzed by comparing the fragments per kb of exon per million fragments mapped (FPKM) values between wild-type and *Erk1/2*$^{oo-/-}$ oocytes. We found a significant difference in transcriptomes between wild-type and *Erk1/2*$^{oo-/-}$ oocytes at the GV/MII stages (Fig. 3A). Compared with the GV oocytes of wild type, we detected 2572 upregulated and 3276 downregulated transcripts in *Erk1/2*$^{oo-/-}$ GV oocytes. Similarly, compared with the MII oocytes of wild type, 5157 significantly upregulated and 1606 downregulated transcripts were detected in *Erk1/2*$^{oo-/-}$ MII oocytes (Fig. 3A). Among the top 1000 most abundant transcripts (10%) in wild-type GV oocytes, 998 transcripts decrease more than 10-fold during GV to MII transition. At GV stage, only 16 and 75 of these transcripts were upregulated and downregulated in *Erk1/2*$^{oo-/-}$ oocytes, respectively (Fig. 3B). However, among the top 10% of abundant transcripts found in GV oocytes of wild-type mice, 455 were upregulated and 23 were downregulated in MII oocytes of *Erk1/2*$^{oo-/-}$ mice, when compared with MII oocytes of wild-type mice (Fig. 3B). These results indicate that half of the top 10% abundant transcripts that should have been degraded during the transition from GV to MII were stabilized in *Erk1/2*$^{oo-/-}$ oocytes.

Moreover, the RNA-seq data were verified using quantitative RT-PCR (qRT-PCR). Fig. 3C,D show the RNA-seq and qRT-PCR results of representative genes that were differentially expressed in wild-type and *Erk1/2*$^{oo-/-}$ oocytes. These transcripts were degraded during MZT of wild-type oocytes, but were stabilized in *Erk1/2*$^{oo-/-}$ oocytes. Significantly upregulated abundant transcripts (*n*=380, FPKM>100) were selected for gene ontology (GO) analysis. We found transcripts of 45 genes that were related to translation (Fig. 3E). It has been reported that the abundant ribosomal transcripts are significantly degraded during oocyte maturation (Su et al., 2007). Our RNA-seq data of wild-type GV/MII oocytes are inconsistent with this observation. The genes that encode the 60S and 40S ribosome subunits are listed in Fig. 3F. Among the 84 transcripts detected in wild-type oocytes, we found that 45 transcripts were upregulated after *Erk1/2* deletion, whereas only eight were downregulated. This finding suggests that ERK1/2 promoted degradation of the ribosomal transcripts during the transition from GV to MII.

ERK1/2 is required for translational activation of multiple CPEB1-targeted maternal mRNAs during oocyte meiotic maturation

As translational activation of *Btg4* mRNA is triggered by ERK1/2 in a CPE-dependent manner, we investigated whether the oocyte maturation-coupled translation of other CPE-containing maternal mRNAs also relied on ERK1/2 activity. Maternally accumulated cyclin B1 and microtubule nucleation factor (TPX2) are responsible for meiotic cell cycle progression and spindle assembly, respectively. However, in oocytes that underwent meiotic maturation in the presence of U0126, the levels of both proteins were lower than normal (Fig. 4A). Immunofluorescence results also showed that TPX2 protein is significantly accumulated onto the spindle of normal MII oocytes, but was absent or considerably downregulated on the distorted spindle of ERK1/2-inhibited oocytes (Fig. 4B). Poly(A) tail assay demonstrated that the poly(A) tails of multiple CPE-containing mRNAs, including

Development (2017) 144, 452-463 doi:10.1242/dev.144410

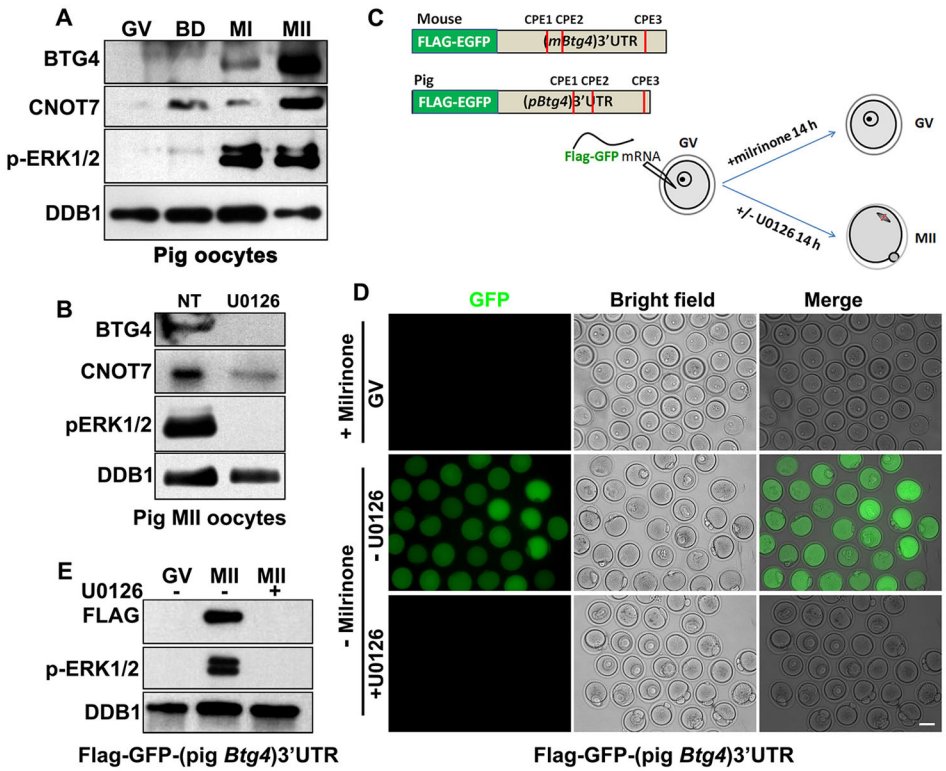

Fig. 1. Regulation of pig BTG4 protein translation during oocyte maturation. (A) Accumulation of BTG4, CNOT7 and phosphorylated ERK1/2 (pERK1/2) in pig oocytes during meiotic maturation. DDB1 was blotted as a loading control. In A,B,E, total proteins from 100 oocytes were loaded in each lane. (B) Western blot results showing levels of phosphorylated ERK1/2 as well as BTG4 and CNOT7 expression in pig MII oocytes with or without U0126 (20 µM) treatment. (C) Diagram of reporter constructs used to determine mouse and pig *Btg4* 3′-UTR activity. CPE, cytoplasmic polyadenylation element. (D,E) Fluorescence microscopy (D) and western blot (E) analysis showing that U0126 blocked the expression of FLAG-GFP fused with pig *Btg4*3′-UTR in mouse oocytes. More than 50 oocytes of each experimental group were observed in D. Scale bar: 50 µm.

Tpx2, *Ccnb1* and *Tex19.1*, were elongated during the GV-to-MI progression. However, this effect was blocked by U0126 (Fig. 4C). In addition, we conducted qRT-PCR for CPE-containing transcripts that were reverse transcribed using oligo-dT or random primers. Oligo-dT favorably mediates the RT reaction of transcripts containing long poly(A) tails, but random primers do not have this preference. Therefore, the ratio changes of qRT-PCR results obtained from oligo-dT- versus random primer-mediated RT

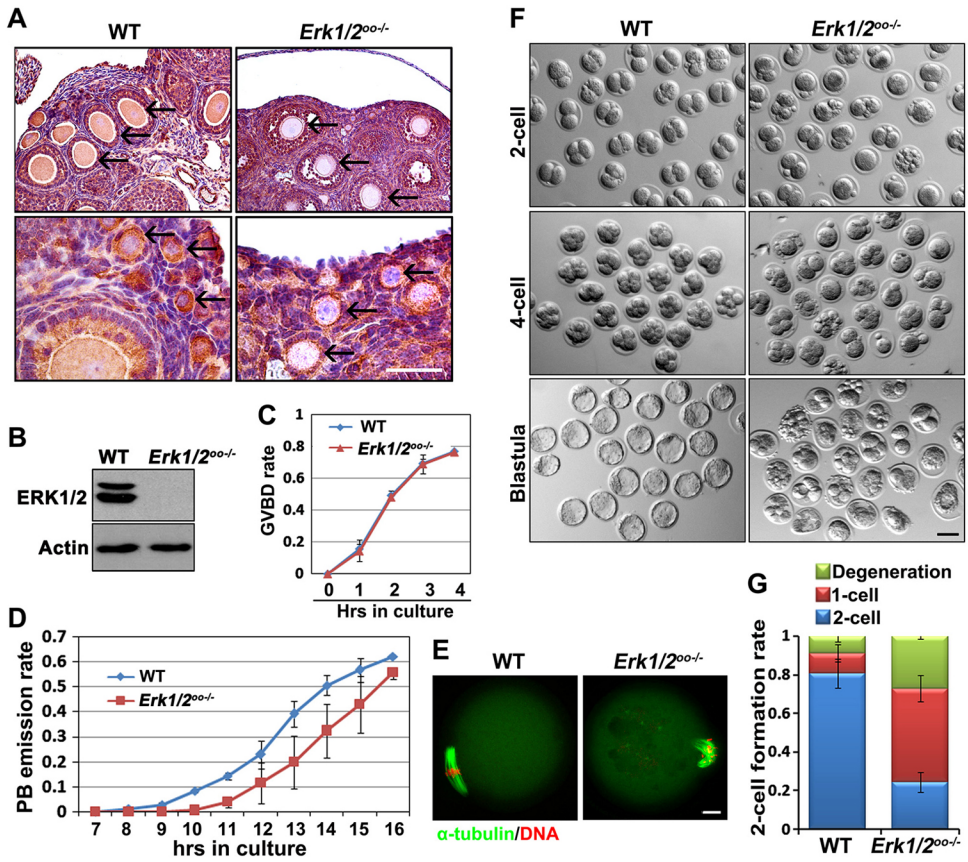

Fig. 2. Phenotype analyses of ERK1/2-deleted oocytes. (A) Immunohistochemistry results showing that ERK1/2 is ubiquitously expressed in the ovaries of wild-type mice, but is absent in the oocytes of *Erk1/2*$^{oo-/-}$ mice, at postnatal day (P) 23. Scale bar: 50 µm. (B) Western blot showing ERK1/2 levels in GV oocytes of wild-type and *Erk1/2*$^{oo-/-}$ mice at P23. β-Actin was blotted as a loading control. Total proteins from 100 oocytes were loaded in each lane. (C) Comparison of GVBD kinetics in cultured oocytes of wild-type and *Erk1/2*$^{oo-/-}$ mice (n=194 for each genotype). (D) Kinetics of polar body emission (PBE). Oocytes that underwent GVBD within 2 h of release from ovaries were selected and cultured further (n=200 for each genotype). Error bars indicate s.e.m. (E) Representative images of immunofluorescent staining for spindle (green) and DNA (red) in wild-type and *Erk1/2*$^{oo-/-}$ oocytes at MII stages. Scale bar: 10 µm. More than 50 oocytes were observed for each genotype. (F) Representative images of 2-cell and 4-cell embryos, and blastocysts collected from wild-type and *Erk1/2*$^{oo-/-}$ mice 44, 60 and 96 h after hCG injection, respectively. Scale bar: 50 µm. (G) Percentages of 1-cell, 2-cell or degenerated embryos collected from wild-type and *Erk1/2*$^{oo-/-}$ mice 44 h after hCG injection. n>50 for each genotype. Error bars indicate s.e.m.

Development (2017) 144, 452-463 doi:10.1242/dev.144410

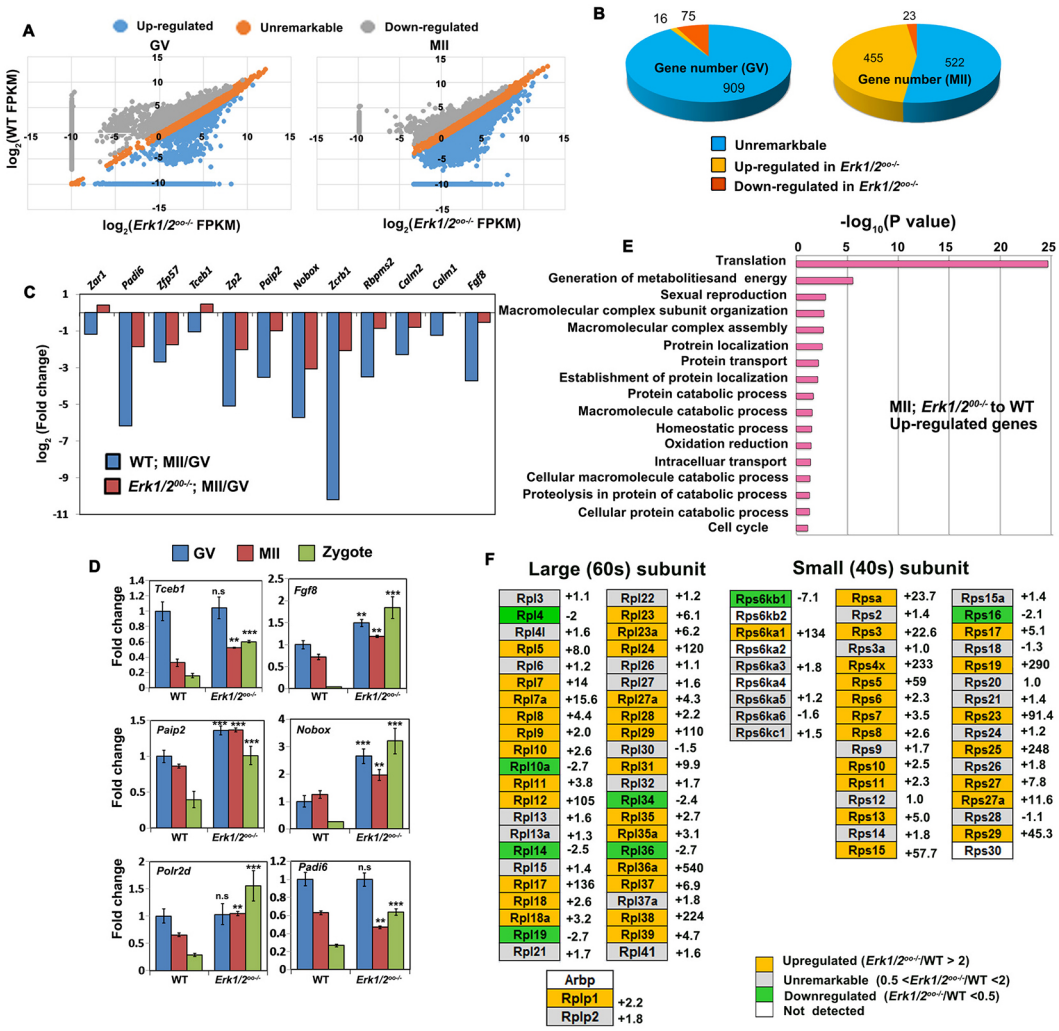

Fig. 3. The mRNA expression profiles in wild-type and *Erk1/2*$^{oo-/-}$ oocytes. (A) Profile of an *Erk1/2*$^{oo-/-}$/wild-type ratio of log2 transformed gene expression levels (FPKMs) in GV and MII oocytes. The number of upregulated [FC(*Erk1/2*$^{oo-/-}$/WT)≥2, P<0.05] and downregulated [FC(*Erk1/2*$^{oo-/-}$/WT)≤0.5, P<0.05] abundant transcripts at the GV and MII stages are shown. (B) The number of transcripts of upregulated (orange), downregulated (red) and unremarkable genes (blue) in the top 10% FPKMs of wild-type GV oocytes. (C) RNA-seq results of selected transcripts [log2(fold change)] in GV and MII oocytes from wild-type and *Erk1/2*$^{oo-/-}$ mice. (D) Quantitative RT-PCR results (with three repeats) of selected transcripts (fold change) in GV/MII oocytes and zygotes from wild-type and *Erk1/2*$^{oo-/-}$ mice. Error bars indicate s.e.m.; **P<0.01 and ***P<0.001 when compared with samples from wild type at the same developmental stage using two-tailed Student's *t*-test. n.s., non-significant. (E) Gene ontology analysis of differentially expressed transcripts [FC(*Erk1/2*$^{oo-/-}$/WT)>2, FPKM>100] in MII oocytes. Enriched gene ontology terms were conducted using DAVID. (F) Changes in transcripts encoded for ribosomal proteins between wild-type and *Erk1/2*$^{oo-/-}$ MII oocytes. The fold changes are listed to the right of the boxes. '+' and '–' indicate upregulation and downregulation by *Erk1/2*-deletion, respectively.

reactions also reflect the poly(A) tail length changes of given maternal transcripts (Moore et al., 1996). As shown in Fig. 4D, oligo-dT mediated more favorable reverse transcription of CPE-containing transcripts (*Dazl*, *Tpx2*, *Ccnb1*, *Btg4* and *Cnot7*), but not of *Gapdh*, in MI oocytes when compared with GV oocytes (wild type). However, U0126 inhibited the oligo-dT-favored reverse transcriptions, indicating that ERK1/2 regulates the poly(A) tail elongation of these mRNAs.

Deleted in azoospermia-like (DAZL) is a CPEB1-downstream factor that mediates maternal mRNA translation in mouse oocytes (Chen et al., 2011). The 3′-UTR of *Dazl* mRNA contains four putative CPEs that bind with CPEB1. *Dazl* mRNA exhibited high levels of polyadenylation at the MI stage (Fig. 4C,D). To test whether ERK1/2 activity is also required for the translational activation of *Dazl* mRNA, we cloned the *Dazl* 3′-UTR from mouse, fused it with Flag-GFP, *in vitro* transcribed it into mRNAs [FLAG-GFP-(*Dazl*)3′-UTR], and injected them into GV oocytes. The experimental strategy is similar to that of the *Btg4* 3′-UTR reporter (Fig. 2C). After an overnight culture, GFP signals were detected in mature oocytes, but not in oocytes that were arrested at the GV stage using milrinone (Fig. 4E). U0126 blocked the translation of injected FLAG-GFP-(*Dazl*)3′-UTR mRNA (Fig. 4E). These observations were confirmed by western blotting of the translated Flag-GFP (Fig. 4F), indicating that the accumulation of DAZL protein in maturing mouse oocytes relies on ERK1/2 activity. Collectively, these results indicate that ERK1/2 targets the 3′-UTR of multiple CPE-containing maternal mRNAs and triggers their translational activation during oocyte meiotic maturation.

ERK1/2 is required for CPEB1 phosphorylation and degradation after oocyte meiotic resumption

In the following experiment, we investigated whether ERK1/2 triggers maternal mRNA translation by modulating CPEB1 in mouse oocytes. CPEB1 protein was present in GV oocytes, and was degraded between

Development (2017) 144, 452-463 doi:10.1242/dev.144410

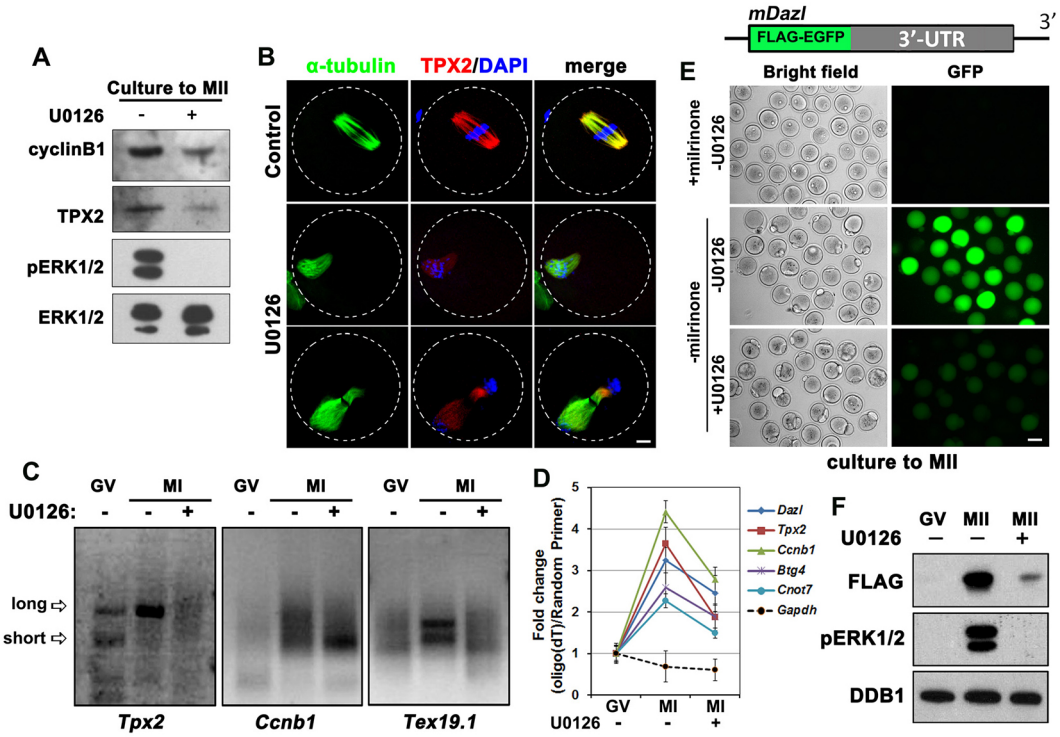

Fig. 4. Role of ERK1/2 in triggering the translational activation of CPE-containing mRNAs in mouse oocytes. (A) Western blot results showing levels of indicated proteins in wild-type oocytes at MII stages, with or without U0126 (20 µM) treatment. Total proteins from 100 oocytes were loaded in each lane. (B) Representative images of immunofluorescent staining for α-tubulin (green) and TPX2 (red) in wild-type oocytes at MII stages with or without U0126 treatment. More than 50 oocytes in each experimental group were observed. Scale bar: 10 µm. (C) Representative poly(A) tail assay results from more than three repeats showing that U0126 treatment blocked poly(A) tailing of indicated mRNAs in MI oocytes. (D) Results of comparing oligo-dT with random primer for RT-PCR showing that U0126 treatment blocked poly(A) tailing of multiple CPE-containing maternal mRNAs in MI oocytes. (E,F) Fluorescence microscopy (E) and western blot (F) results showing that U0126 blocked the expression of FLAG-GFP fused with *Dazl* 3′-UTR in mouse oocytes. More than 50 oocytes in each experimental group were observed (E) and total proteins from 60 oocytes were loaded in each lane (F). Scale bar: 50 µm.

4 and 6 h at meiosis resumption (Fig. 5A). An upshift band of CPEB1 was detected 4 h after meiotic resumption, coinciding with the phosphorylation activation of ERK1/2 at the same time point (Fig. 5A). When protein degradation was blocked, using the 26S proteosome MG132, the CPEB1 upshift was more clearly demonstrated (Fig. 5B). Western blots following phosphate affinity SDS-PAGE (Phos-tag-WB) further demonstrated that CPEB1 was phosphorylated before its degradation (Fig. 5C). The MEK1/2 inhibitor U0126 blocked both upshift and degradation of CPEB1 in maturing oocytes (Fig. 5A,B). Phos-tag-WB results also showed that GVBD-coupled CPEB1 phosphorylation was significantly inhibited by U0126 (Fig. 5C). CPEB1 phosphorylation and degradation were also impaired in *Erk1/2*$^{oo-/-}$ oocytes (Fig. 5D). These data demonstrate that ERK1/2 activity was required for triggering CPEB1 phosphorylation and degradation after oocyte meiotic resumption.

CPEB1 is phosphorylated and partially degraded during mouse oocyte meiotic maturation

To determine the CPEB1 phosphorylation sites in maturing oocytes, we focused on the two conserved SP motifs in mammalian CPEB1 (serine 181 and 207, both putative ERK1/2 phosphorylation sites) (Fig. 5E) and mutated the two serine residues to alanine either separately (CPEB1-S181/A or CPEB1-S207/A) or together (CPEB1-2A). We injected mRNAs encoding wild-type and mutated CPEB1 in oocytes arrested at the GV stage using milrinone. Following an overnight culture, oocytes were released from GV arrest by being transferred to milrinone-free medium. At 6 h following meiotic resumption, CPEB1 phosphorylation was decreased by either the S181/A or S207/A mutations, and was more significantly inhibited in CPEB1-2A mutants (Fig. 5F). Furthermore, we tested whether phosphorylation at S181 and S207 also regulates CPEB1 stability during meiotic maturation. Wild-type and mutated CPEB1 were expressed at a comparable level at GV stage (Fig. 5G). At 6 h after release from GV arrest, most wild-type CPEB1 proteins were degraded, whereas the CPEB1 mutant forms were stabilized, with CPEB1-2A being the most stable form (Fig. 5G).

The ubiquitin-dependent degradation of CPEB in maturing *Xenopus* oocytes requires a conserved PEST (Pro/Glu/Ser/Thr) sequence that binds with CRL1-βTrCP ubiquitin E3 ligase (Fig. 5E). Deleting the conserved PEST sequence in mouse CPEB1 (CPEB1-ΔPEST) prevented its binding with βTrCP, the substrate adaptor of CRL1 (Fig. 5H). Overexpression of βTrCP induced polyubiquitylation of CPEB1-WT, but not CPEB1-ΔPEST (Fig. 5I). The PEST sequence is spanned by S181 and S207 (Fig. 5E). CPEB1-2A neither bound with βTrCP, nor showed increased polyubiquitylation after βTrCP overexpression (Fig. 5H,I). Collectively, these results indicate that CRL1$^{\beta TrCP}$ mediates CPEB1 degradation in maturing mouse oocytes, and phosphorylation of S181 and S207 facilitates CPEB1 degradation by increasing its binding with βTrCP.

The activation and partial degradation of CPEB1 through phosphorylation is essential for meiotic maturation

In the following experiments, we investigated whether ERK1/2-triggered CPEB1 phosphorylation and degradation play a key role in

Development (2017) 144, 452-463 doi:10.1242/dev.144410

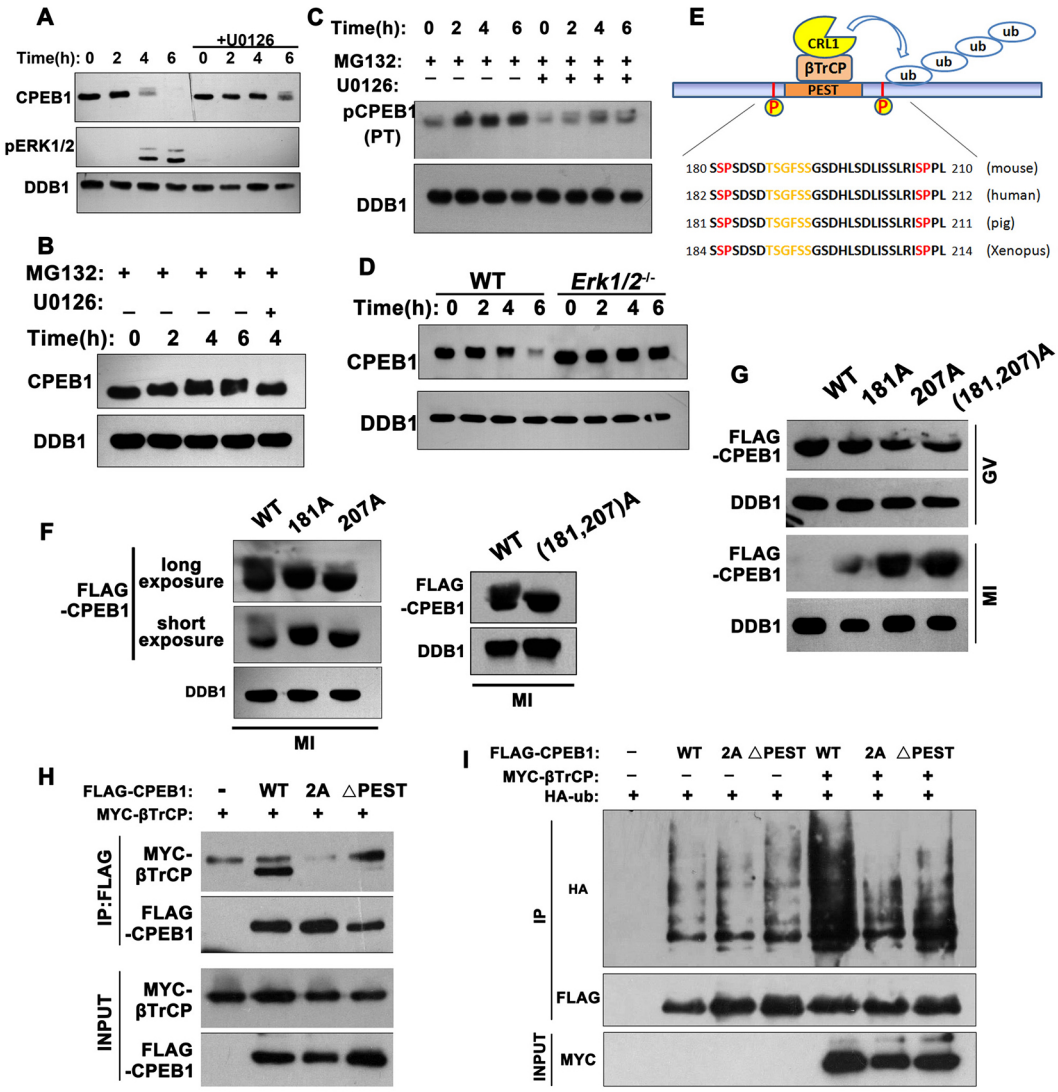

Fig. 5. Regulation of CPEB1 phosphorylation and degradation by ERK1/2 in mouse oocytes. (A) Levels of CPEB1 at indicated time points after meiotic resumption, with or without U0126 (20 μM) treatment. In A-D,F,G, total proteins from 50 oocytes were loaded in each lane. DDB1 was blotted as a loading control. (B) Western blot results showing phosphorylation of CPEB1 after meiotic resumption, with or without U0126 treatment. MG132 (10 μM) was added to culture medium to prevent CPEB1 degradation. (C) Western blot following phosphate affinity SDS-PAGE (Phos-tag-WB) results showing the phosphorylation of CPEB1 after meiotic resumption, with or without U0126 treatment. (D) Levels of CPEB1 in wild-type and *Erk1/2*$^{oo-/-}$ oocytes after meiotic resumption. (E) Putative phosphorylation sites and the PEST sequence in vertebrate CPEB1. (F,G) Western blot using anti-FLAG antibody showing band shift (F) and levels (G) of CPEB1 in maturing mouse oocytes. mRNAs encoding Flag-tagged wild-type and mutated CPEB1 were injected into GV-arrested oocytes. Oocytes were allowed to resume meiotic maturation 12 h after microinjection. (H,I) Co-immunoprecipitation (co-IP) results showing interactions between CPEB1 (WT, 2A, ΔPEST) and βTrCP (H), as well as the poly-ubiquitylation of CPEB1 (WT, 2A, ΔPEST) by βTrCP (I). HeLa cells were co-transfected with plasmids encoding indicated proteins, and were lysed for co-IP 48 h after transfections.

oocyte maturation. GV-arrested oocytes were injected with mRNAs encoding CPEB1-WT or mutant proteins, and then allowed to undergo meiotic maturation 10-12 h after injection. Overexpression of CPEB1-WT in GV oocytes was quickly degraded after meiotic resumption, and did not cause any abnormalities (Fig. 5G and Fig. 6A-D). Overexpression of CPEB1-2A or CPEB1-ΔPEST did not affect GVBD (4 h after release from GV arrest), but resulted in decreased PB1 emission rates (12 h after release from GV-arrest) (Fig. 6A). It is noteworthy that the PB1 emission rate of CPEB1-2A-overexpressing oocytes was lower than that of *Erk1/2*$^{oo-/-}$ oocytes, indicating a strong dominant-negative effect (Fig. 6B). Distorted spindles were observed in most CPEB1-2A-overexpressing oocytes (Fig. 6C). TPX2, a microtubule-associated protein that is important for spindle assembly and chromosome alignment, accumulated at the MII spindle of normal oocytes (Fig. 6C). However, the TPX2 signal was undetectable on spindles of CPEB1-2A-overexpressing oocytes (Fig. 6C). Chromosome spreading and immunofluorescence showed that control MII-arrested oocytes contained 20 pairs of sister chromatids, but the CPEB1-2A-overexpressing oocytes still have paired homologous chromosomes (tetrads), indicating impaired chromosome separation in anaphase I (Fig. 6D). Deletion of the PEST sequence stabilized CPEB1 in maturing oocytes (Fig. 6E). Although spindle shape was distorted in CPEB1-ΔPEST-overexpressing oocytes, it was not as severe as that found in CPEB1-2A-overexpressing oocytes; however, the decrease of spindle-localized TPX2 was remarkable (Fig. 6C). In addition, compact chromosomes did not properly align at the equator of the spindles in these oocytes, and homologous chromosome separation

Development (2017) 144, 452-463 doi:10.1242/dev.144410

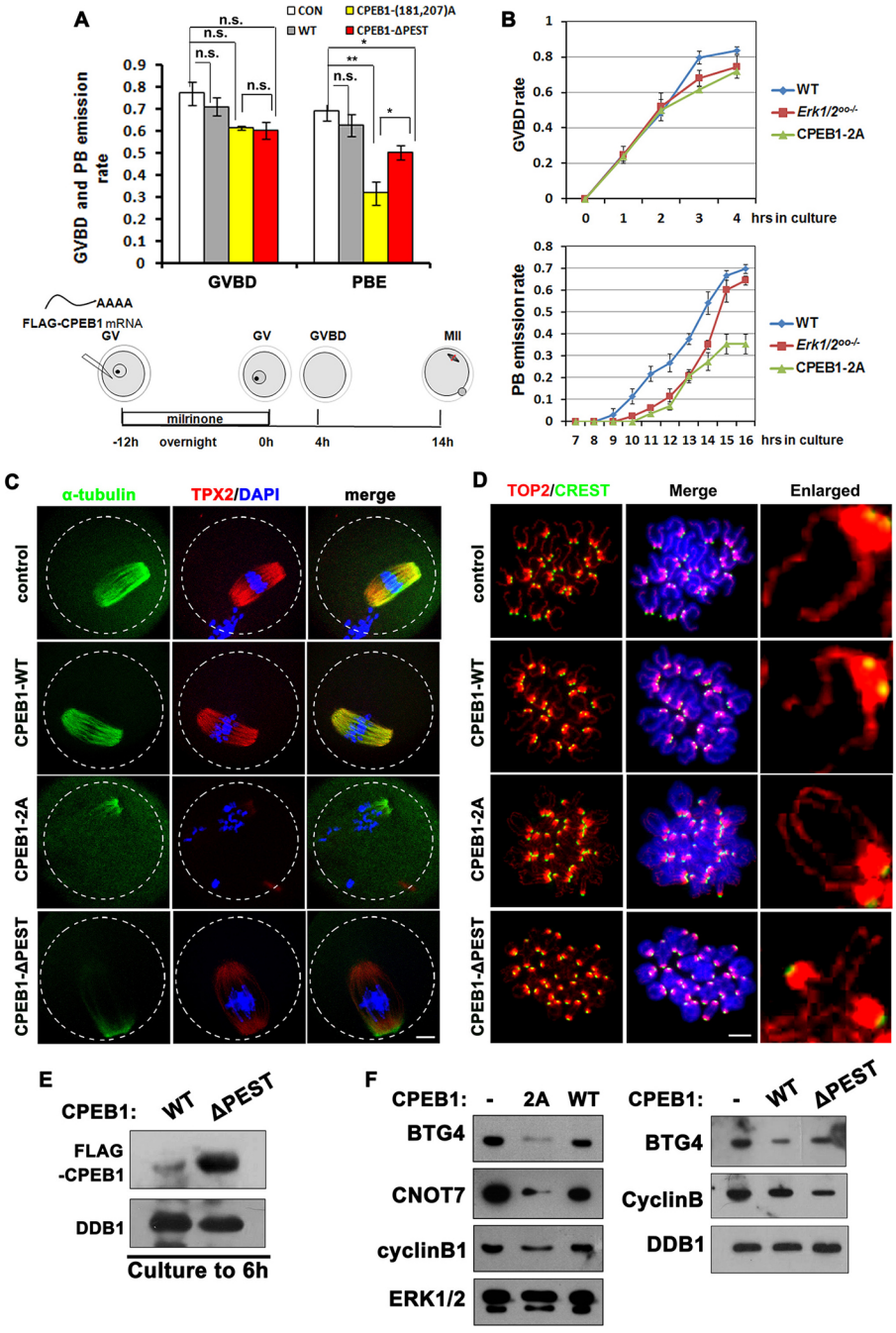

Fig. 6. Effects of CPEB1 expression on oocyte maturation. (A) GVBD and polar body emission (PBE) rates in cultured oocytes injected with wild-type and mutated CPEB1, as demonstrated by the diagram (*n*=200 for each group). Error bars indicate s.e.m.; **P*<0.05, ***P*<0.01 (two-tailed Student's *t*-test). n.s., non-significant. (B) Dynamics of GVBD and PB emission in cultured oocytes of wild-type, *Erk1/2*$^{oo-/-}$ mice and in oocytes injected with CPEB1-2A (*n*=200 for each genotype). Error bars indicate s.e.m. (C) Immunofluorescent staining for α-tubulin (green) and TPX2 (red) in oocytes injected with wild-type and mutated CPEB1, as demonstrated by the diagram in A. More than 50 oocytes in each experimental group were observed. Scale bar: 10 µm. (D) Chromosome spreading and immunofluorescent staining for TOP2 (red) and CREST (green) in oocytes injected with wild-type and mutated CPEB1, as demonstrated by the diagram in A. More than 50 oocytes in each experimental group were observed. Scale bar: 10 µm. (E) Western blot results showing CPEB1 protein levels in oocytes injected with wild-type and PEST sequence-deleted CPEB1 (ΔPEST) 6 h after releasing from GV arrest. Total proteins from 50 oocytes were loaded in each lane. (F) Western blot results showing levels of indicated proteins in oocytes injected with wild-type and mutated CPEB1 14 h after releasing from GV arrest. Total proteins from 100 oocytes were loaded in each lane.

was blocked (Fig. 6C,D). At the molecular level, overexpression of CPEB1-2A or PEST deletion blocked the accumulation of cyclin B1, BTG4 and CNOT7 (Fig. 6F). Taken together, the phosphorylation site- or degradation site-mutated CPEB1 has a dominant-negative effect in preventing bipolar spindle formation and homologous chromosome separation during oocyte maturation, both of which are meiotic events controlled by ERK1/2 in mammalian oocytes.

The CPEB1 downstream translation activator DAZL partially rescues meiosis defects in *Erk1/2*$^{oo-/-}$ oocytes

To further demonstrate that ERK1/2 regulates oocyte maturation by activating CPEB1 and triggering translation of essential maternal mRNAs, we tested whether the CPEB1 downstream protein DAZL could bypass ERK1/2 function, and rescue the meiosis defects seen in ERK1/2-inhibited oocytes. The 3′-UTR of mouse *Btg4* contains four putative DAZL-binding elements (Fig. 7A). When the CPEs in the *Dazl* 3′-UTR were mutated, the translation levels of Flag-GFP-(*Btg4*)3′-UTR were significantly decreased (Fig. 7A). This result indicates that DAZL is required to maintain high levels of BTG4 expression after CPEB1 degradation. Furthermore, when we overexpressed mCherry-DAZL in maturing oocytes cultured with U0126 (Fig. 7B), expression of endogenous BTG4 and CNOT7 was partially rescued at the MII stage (Fig. 7C), confirming that DAZL functions downstream of ERK1/2 and CPEB1. In oocytes that underwent meiotic maturation in the presence of U0126, spindle assembly and TPX2 recruitment were impaired (Fig. 7D,F), and sister chromatids were prematurely segregated (Fig. 7E,G). The expression of exogenous DAZL partially rescued these phenotypes

Development (2017) 144, 452-463 doi:10.1242/dev.144410

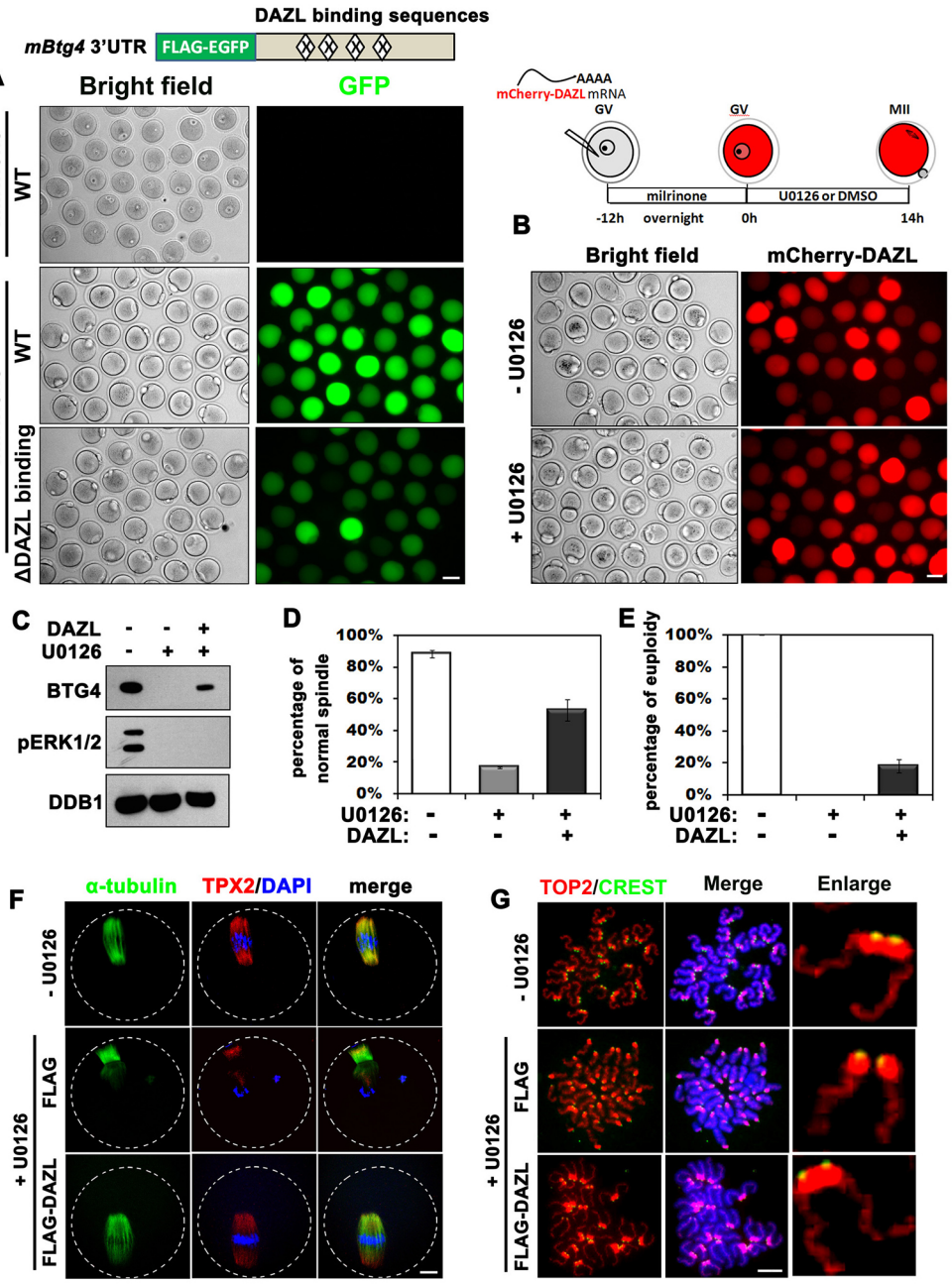

Fig. 7. DAZL partially rescues the oocyte maturation defects caused by ERK1/2 inhibition. (A) Fluorescence microscopy results showing GFP expression driven by wild-type and DAZL-binding site mutated *Btg4* 3′-UTR. Mouse GV oocytes were injected with *in vitro* transcribed Flag-GFP-(*Btg4*)3′UTR mRNA (wild-type or ΔDAZL binding) and cultured for 14 h with or without milrinone. More than 50 oocytes from each experimental group were observed. Scale bar: 50 µm. (B) Fluorescence microscopy results showing expression of mCherry-DAZL. Mouse GV oocytes were injected with *in vitro* transcribed and polyadenylated mRNA encoding mCherry-DAZL, and further cultured with or without U0126 (20 µM). Scale bar: 50 µm. (C) Western blot results showing BTG4 protein expression in U0126-treated oocytes with or without DAZL overexpression. In C-G, oocytes were injected and harvested as illustrated in B, except that a FLAG-DAZL was expressed. Total proteins from 100 oocytes were loaded in each lane. (D,E) Percentage of oocytes with normal spindles (D) and sister chromatid pairs (E). Error bars indicate s.e.m. (F) Immunofluorescent staining results for α-tubulin (green) and TPX2 (red) in oocytes showing that DAZL partially rescued the spindle assembly defect in U0126-treated oocytes. Scale bar: 10 µm. More than 50 oocytes from each experimental group were observed. (G) Chromosome spreading and immunofluorescent staining for TOP2 (red) and CREST (green), showing that DAZL partially prevented premature sister chromatid separation in U0126-treated oocytes. Scale bar: 10 µm.

caused by ERK1/2 inhibition (Fig. 7D-G). Taken together, these results highlight the role of CPEB1 and DAZL in sequentially mediating the function of ERK1/2 in maturing oocytes.

DISCUSSION

CPEB1-mediated mRNA cytoplasmic polyadenylation is crucial to maternal mRNA translation during oocyte maturation. Its targeting sequence CPEs are associated with regulation of the poly(A) tail length, and they are present in the 3′-UTR of many key maternal mRNAs, suggesting that polyadenylation is a regulatory mechanism for the translation of these mRNAs. Both CPEB1 proteins and their target mRNAs were abundantly accumulated in GV-arrested oocytes, yet the polyadenylation and translation of these maternal mRNAs were only activated after meiotic resumption. Until this work, how CPEB1 activity is regulated in mammalian oocytes was unclear.

During *Xenopus* oocyte maturation, two different types of CPEB modifications contribute to translational activation. Phosphorylation of CPEB on Ser174 that occurs at an early stage of maturation is required for early activation of a class of mRNAs such as those encoding Mos (Martinez et al., 2005). However, a large fraction (70-90%) of CPEB proteins undergoes a CRL1-βTrCP-dependent degradation in meiosis I (Reverte et al., 2001). This degradation causes a change in the CPEB/CPE ratio and results in activation of another class of mRNAs, thereby driving entry into meiosis II.

Whereas the phosphorylation of mouse CPEB1 has been poorly studied, multiple MPAK and CDK1 phosphorylation sites have been identified in *Xenopus* CPEB. Among these, S210 phosphorylation by CDK1 is sufficient to target CPEB1 for destruction; however, one or more other proline-directed serine phosphorylations may also be involved (Mendez et al., 2002). Another study showed that MAPK activated CPEB (measured by

Development (2017) 144, 452-463 doi:10.1242/dev.144410

Mos mRNA polyadenylation and translation) by directly phosphorylating it on four residues (T22, T164, S184 and S248) (Keady et al., 2007). Among these, S184 and S210 span the PEST sequence and are highly conserved in mammalian species (corresponding to S181 and S207 in mouse CPEB1). In this study, we provide evidence that ERK1/2-triggered phosphorylation at these two sites is crucial for CPEB1 degradation and oocyte maturation. The phosphorylation of these sites also facilitated the CPEB1-βTrCP binding. However, because preventing CPEB1 phosphorylation also blocked its degradation, we could not distinguish the specific roles of these two tightly associated biochemical events (CPEB1 phosphorylation and degradation). In addition, CPEB1-2A overexpression has a stronger effect on the PB emission than *Erk1/2* deletion, suggesting that protein kinase(s) other than ERK1/2 may also regulate the phosphorylation of CPEB1 at S181 and S207.

By activating CPEB1, ERK1/2 triggers translational activation of multiple CPE-containing maternal mRNAs, including those encoding BTG4, TPX2 and DAZL, which are known to be essential for oocyte maturation and MZT (Brunet et al., 2008; Chen et al., 2011; Yu et al., 2016b). We provide evidence that the insufficient accumulation of these maternal factors is the primary reason for the developmental defects seen in ERK1/2-inhibited oocytes. Studies on mouse oocytes indicate that DAZL functions as a CPEB1-downstream translational activator, and several putative targets, including *Tex19.1*, *Tpx2* and *Dazl* itself, have been identified (Sousa Martins et al., 2016). In this study, we add *Btg4* to the list of DAZL-regulated maternal transcripts. DAZL maintains the translation of *Btg4* mRNAs in oocytes during late maturation by targeting four DAZL-binding elements in its 3′-UTR, when CPEB1 has been degraded. Using a 3′-UTR reporter assay, we also demonstrated that the translational activation of *Dazl* mRNA was oocyte maturation coupled and depended on ERK1/2 activity.

DAZL function in oocyte maturation has previously been studied. Injection of *Dazl* morpholinos in GV oocytes reduced the number of oocytes that complete meiosis I (measured as polar body extrusion) and disrupted the spindle assembly at MII. Chromosome condensation and separation are also disrupted (Chen et al., 2011). These phenotypes mimicked several aspects of ERK1/2 knockout or inhibition in oocytes, suggesting that DAZL may be a key mediator of ERK1/2 function. Indeed, overexpression of DAZL in ERK1/2-inhibited oocytes partially rescued the oocyte maturation defects, including spindle assembly, MII arrest maintenance (measured as sister chromatid cohesion) and translational activation (measured as TPX2 and BTG4 accumulation). These results highlighted that the major function of ERK1/2 in oocytes was mediated by sequentially translated maternal factors, including DAZL, TPX2 and BTG4. These factors function in parallel with the directly phosphorylated targets of ERK1/2, such as the microtubule-associated target proteins MISS and DOC1R.

TPX2 is localized on spindle microtubules and activates Aurora A, an indispensable regulator of centrosome and spindle pole assembly (Eckerdt et al., 2009). In addition, TPX2 induces microtubule nucleation near chromosomes and facilitates spindle pole organization (Helmke and Heald, 2014). Our current study provides evidence that TPX2 accumulation on the meiotic spindle is severely impaired in ERK1/2-deficient oocytes, as its protein translation requires DAZL. *Tpx2* mRNA depletion causes phenotypic changes very similar to those we observed with *Erk1/2* knockout, including disruption of spindle assembly and failure of chromosome condensation. Therefore, defective spindle function assembly caused by inadequate levels of TPX2 protein is likely to contribute to the defects we observed after ERK1/2 inhibition or knockout.

We report for the first time that ERK1/2 is essential for MZT, in addition to its function in oocyte meiotic maturation. Although *Erk1/2*$^{oo-/-}$ oocytes have defects in spindle assembly and chromosome alignment, they are still able to develop to MII and be fertilized. However, the zygotes derived from these oocytes fail to develop beyond the 2-cell stage, and mimicked the phenotype of the *Btg4* knockout. During meiotic maturation, activated ERK1/2 and CPEB1 trigger polyadenylation and translation of many maternal mRNAs, including those encoding *Btg4* and *Cnot7*. The accumulated BTG4 and CNOT7 proteins in turn, mediate maternal mRNA deadenylation and degradation (Liu et al., 2016; Yu et al., 2016b). Therefore, a negative-feedback regulation mechanism is formed to ensure transient, but not prolonged, translation of proteins that are crucial for oocytes and zygotes. The function of ERK1/2 in regulating maternal mRNA translation and degradation during oocyte maturation and MZT is summarized in Fig. 8.

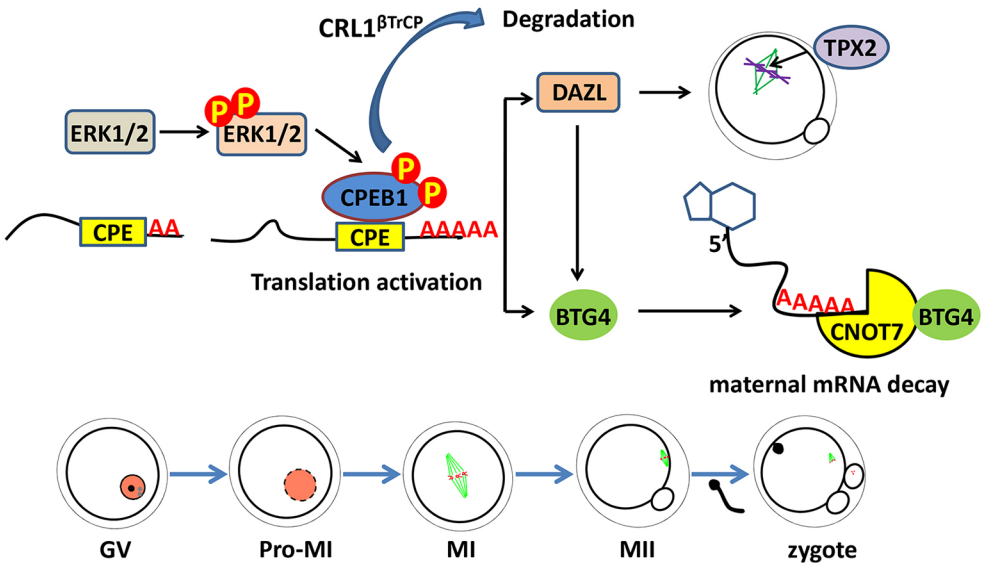

Fig. 8. The role of ERK1/2 in triggering maternal mRNA translation during mouse oocyte maturation. Upon oocyte meiotic resumption, ERK1/2 is activated by upstream kinases and triggers CPRB1 phosphorylation and CRL1^{βTrCP}-dependent degradation. The phosphorylation and partial degradation of CPEB1 stimulate polyadenylation and translational activation of maternal mRNAs, including *Dazl* and *Btg4*. The accumulated DAZL proteins lead to further translational activation of maternal mRNAs such as *Tpx2* and *Btg4*, whereas BTG4 and CNOT7 target polyadenylated maternal mRNAs to degradation. By initiating these hierarchical maternal mRNA regulation processes, ERK1/2 functions as a meiotic cell cycle-coupled licensing factor of maternal mRNA translation.

Development (2017) 144, 452-463 doi:10.1242/dev.144410

Our oocyte RNA sequencing and GO analyses indicated that ERK1/2-targeted transcripts were remarkably enriched for transcripts of genes associated with protein translation. Interestingly, this result coincides with previous reports. By microarray analyses, Su and colleagues demonstrated that the destruction of transcripts during the GV-to-MII transition is selective rather than promiscuous in mouse oocytes (Su et al., 2007). In particular, transcripts associated with meiotic arrest and the progression of oocyte maturation, such as oxidative phosphorylation, energy production and protein synthesis, were dramatically degraded. Selective degradation of these maternal transcripts is a prerequisite for transition from oocyte meiosis to blastomere mitosis, as well as transcriptional activation of the zygotic genome (Yu et al., 2016a,b). Aberrant degradation or maintenance of some classes of transcripts during oocyte maturation could be deleterious to oocyte quality and affect developmental competence, as we demonstrated in ERK1/2- and CPEB1-inhibited oocytes in this study.

MATERIALS AND METHODS

Animals

Erk1$^{-/-}$, *Erk2*$^{flox/flox}$ and *Gdf9-Cre* mice have been previously reported (Fan et al., 2009; Zhang et al., 2015). All mouse strains had a C57B6 background. Wild-type C57B6 mice were obtained from the Zhejiang Academy of Medical Science, China. Mice were maintained under SPF conditions in a controlled environment of 20-22°C, with a 12/12 h light/dark cycle, 50-70% humidity and food and water provided *ad libitum*. Animal care and experimental procedures were conducted in accordance with the Animal Research Committee guidelines of Zhejiang University.

In vitro transcription and preparation of mRNAs for microinjections

To prepare mRNAs for microinjection, expression vectors were linearized and subjected to phenol/chloroform extraction and ethanol precipitation. The linearized DNAs were *in vitro* transcribed using the SP6 mMESSAGEmMACHINE Kit (Invitrogen, AM1450) following the manufacturer's instructions. mRNAs were recovered by lithium chloride precipitation and resuspended in nuclease-free water.

Microinjection of oocytes

For microinjection, fully grown GV oocytes were harvested in M2 medium with 2 µM milrinone to inhibit spontaneous GVBD. All injections were performed using an Eppendorf Transferman NK2 micromanipulator. Denuded oocytes were injected with 5 to 10 pl samples per oocyte. After injection, oocytes were washed and cultured in M16 medium plus 2 µM milrinone at 37°C with 5% CO_2.

Superovulation and fertilization

Female mice (21-23 days old) were intraperitoneally injected with 5 IU of PMSG (Ningbo Sansheng Pharmaceutical, China). After 44 h, mice were injected with 5 IU of hCG (Ningbo Sansheng Pharmaceutical, China). After an additional 16 h, oocyte/cumulus masses were surgically removed from the oviducts and the numbers of oocytes were counted after digestion with 0.3% hyaluronidase (Sigma-Aldrich). Oocyte images were acquired using a Nikon SMZ1500 stereoscope. To obtain early embryos, female mice were mated with 10- to 12-week-old wild-type males. Successful mating was confirmed by the presence of vaginal plugs. Embryos were harvested from oviducts at the indicated times post-hCG injection.

Oocyte and embryo culture

Mice at 21 days of age were injected with 5 IU of PMSG and humanely euthanized 44 h later. Oocytes at the GV stage were harvested in M2 medium (M7167; Sigma-Aldrich) and cultured in mini-drops of M16 medium (M7292; Sigma-Aldrich) covered with mineral oil (M5310; Sigma-Aldrich) at 37°C in a 5% CO_2 atmosphere. In some experiments, U0126 (20 µM) was added to the culture media to inhibit ERK1/2 activation. Zygotes were harvested from fertilized females 24 h after the hCG injection and cultured in KSOM medium (Millipore).

Immunohistochemistry

PBS-buffered formalin-fixed, paraffin wax-embedded ovary samples were sectioned (5 µm) for immunohistochemistry. Sections were deparaffinized and rehydrated. Primary antibodies were applied at suitable dilutions (Table S1) at room temperature for 1 h, and then incubated with biotinylated secondary antibodies for 30 min. Sections were then stained using Vectastain ABC and DAB peroxidase substrate kits (Vector Laboratories). Antibodies used in this study are listed in Table S1.

Confocal microscopy of mouse oocytes and embryos

Oocytes or embryos were fixed in PBS-buffered 4% paraformaldehyde (PFA) for 30 min at room temperature, followed by permeabilization with 0.2% Triton X-100. After blocking with 1% BSA in PBS, oocytes were incubated with primary antibodies diluted in blocking solution at room temperature for 1 h. After three washes with PBS, oocytes were labeled with secondary antibodies for 45 min, and then counterstained with 5 µg/ml of 4′,6-diamidino-2-phenylindole (DAPI) for 10 min. Oocytes were mounted on glass slides using SlowFade Gold Antifade Reagent (Life Technologies) and examined under a confocal laser scanning microscope (LSM 710, Carl Zeiss).

Chromosome spreading and immunofluorescence

ZP-free oocytes were fixed in a solution containing 1% paraformaldehyde, 0.15% Triton X-100 and 3 mmol/l DTT (Sigma-Aldrich) on glass slides for 30 min and air dried. Immunofluorescent staining was performed as in oocytes described above.

Western blot analysis

Oocytes were lysed with SDS sample buffer and heated for 5 min at 95°C. Total oocyte proteins were separated by SDS-PAGE and electrophoretically transferred to PVDF membranes (Millipore), followed by blocking in TBST containing 5% defatted milk (Becton Dickinson) for 30 min. After probing with primary antibodies, the membranes were washed in TBST, incubated with an HRP-linked secondary antibody (Jackson ImmunoResearch Laboratories) for 1 h, followed by three washes with TBST. Bound antibodies were detected using the Super Signal West Femto maximum sensitivity substrate (Thermo Fisher Scientific). The primary antibodies and dilution factors used are listed in Table S1.

Phos-tag SDS-PAGE analysis

Oocytes were lysed with SDS sample buffer and heated for 5 min at 95°C. Gels for Phos-tag SDS-PAGE consisted of 50 µM Phos-tag acrylamide (Wako, AAL-107) and 100 µM $MnCl_2$ other than SDS-PAGE. Total oocyte proteins were separated by Phos-tag SDS-PAGE. Gels were washed in the transfer buffer containing 10 mM EDTA and then electrophoretically transferred to PVDF membranes (Millipore). The following steps were performed as described in the western blot analysis section.

Cell culture, plasmid transfection and immunoprecipitation

HeLa cells were obtained from ATCC and were recently authenticated and tested for contamination. Cells were grown in DMEM (Invitrogen) supplemented with 10% fetal bovine serum (FBS; Hyclone) and 1% penicillin-streptomycin solution (Gibco) at 37°C in a humidified 5% CO_2 incubator. Mouse *Cpeb1* and *βTrCP* cDNAs were PCR amplified from a mouse ovarian cDNA pool and cloned into pCS2- or pcDNA-based eukaryote expression vectors. Transient plasmid transfection was carried out using Lipofectamine 2000 (Invitrogen). After a 48 h transfection, cells were lysed in lysis buffer [50 mM Tris-HCl (pH 7.5), 150 mM NaCl, 10% glycerol, and 0.5% NP-40]. After centrifugation, the supernatant was subjected to immunoprecipitation with different affinity gels (Sigma). After incubation at 4°C for 4 h, beads were washed with lysis buffer. SDS sample buffer was added to the beads and the eluted proteins were used for western blot analysis.

Development (2017) 144, 452-463 doi:10.1242/dev.144410

Poly(A) tail assay

Total RNA was isolated from oocytes at indicated stages using the RNeasy Mini Kit (Qiagen). The RNA was then hybridized with or without oligodT (20) before RNaseH treatment. RNA was purified and reacted with 5 mM GTP and ITP in RNase-free water for 1 h at 37°C using yPoly(A) polymerase (Affymetrix). Reverse transcription was performed using the SuperScript III Kit (Invitrogen) with C10T2 DNA primer (5′ CCC CCCCCC CTT 3′). The products were used in a PCR reaction with gene-specific primers (Table S2) and PAT2 (5′ CA GGA AAC AGC TAT GAC CCC CCCCCC CTT 3′) under the following conditions: 30 s at 94°C, 60 s at 56°C and 60 s at 72°C. PCR products were analyzed on a 2.5% agarose gel.

RNA isolation and library construction

GV and MII oocytes were collected from wild-type and *Erk1/2*$^{oo-/-}$ mice (300 per sample). Total RNA was extracted from each sample using the RNeasy Mini Kit (Qiagen) according to the manufacturer's protocol. In the initial step, we spiked 2×10^6 mRNA-GFP and 2×10^6 mRNA-RFP, transcribed *in vitro*, into each lysed sample for RNA isolation. Extracted total RNA was used to prepare a sequencing library using the TruSeq RNA Sample Prep Kit V2 (Illumina). Briefly, mRNA was purified with Oligo d (T)-25 beads, fragmented, and then reverse transcribed. The second strand was then synthesized with random primers in succession. Afterwards, double-stranded cDNA was subjected to end repair, A-tailing, adaptor ligation and PCR amplification of 10-12 cycles in order to obtain the library.

RNA-Seq data analysis

We aligned RNA-seq reads, sequenced by IlluminaHiseq 2500, to *Mus musculus* UCSC mm9 references with the Tophat software (http://tophat.cbcb.umd.edu/) and calculated the FPKM of each gene using Cufflinks (http://cufflinks.cbcb.umd.edu). The amount of total mRNA was calculated based on the FPKM of exogenous GFP and RFP. The expression level of each gene was calculated as its FPKM normalized to the FPKM of GFP/RFP. The top 10% transcripts at GV stage in wild type were selected, and the number of upregulated (FPKM+0.1, *Erk1/2*$^{oo-/-}$/WT>2) and downregulated (FPKM+0.1, *Erk1/2*$^{oo-/-}$/WT<0.5) transcripts were compared at GV and MII stage, respectively. DEGs (differentially expressed genes) were assessed using cuffdiff at a P value of <0.05 and FC (fold change) of >2 or <0.5. GO analysis for enrichment of DEGs was determined using the Database for Annotation, Visualization and Integrated Discovery (DAVID).

RNA isolation and real-time RT-PCR

Total RNA was extracted using the RNeasy Mini Kit (Qiagen) according to the manufacturer's instructions. Real-time RT-PCR analysis was performed using a Power SYBR Green PCR Master Mix (Applied Biosystems, Life Technologies) and an Applied Biosystems 7500 Real-Time PCR System. Relative mRNA levels were calculated by normalizing to the levels of endogenous β-actin mRNA (internal control) using Microsoft Excel. The relative transcript levels of samples were compared with the control, and the fold changes are demonstrated. For each experiment, qPCR reactions were carried out in triplicate. Primer sequences are listed in Table S2.

Statistical analysis

Results are given as mean±s.e.m. Each experiment included at least three independent samples and was repeated at least three times. Results for two experimental groups were compared using two-tailed unpaired Student's *t*-tests. Statistically significant values are indicated as follows: *P<0.05, **P<0.01 and ***P<0.001.

Competing interests

The authors declare no competing or financial interests.

Author contributions

H.-Y.F. and Y.-L.Z. conceived the project and designed the experiments. Q.-Q.S. and X.-X.D. performed and analyzed the bulk of the experiments. Y.D., Y.-L.Z. and F.T. performed and analyzed the RNA-seq and WBGS. J.P.L. helped to perform the experiments. Q.-Q.S. wrote the manuscript and H.-Y.F. and Y.-L.Z. revised it.

Funding

This study is funded by the National Key Research and Development Program of China (2016YFC1000600) and by the National Natural Science Foundation of China (31528016, 91519313, 31371449, 31671558).

Data availability

The RNA-seq data have been deposited at Gene Expression Omnibus under series accession GSE92317 (http://www.ncbi.nlm.nih.gov/geo/query/acc.cgi?acc=GSE92317).

Supplementary information

Supplementary information available online at
http://dev.biologists.org/lookup/doi/10.1242/dev.144410.supplemental

References

Brunet, S., Dumont, J., Lee, K. W., Kinoshita, K., Hikal, P., Gruss, O. J., Maro, B. and Verlhac, M.-H. (2008). Meiotic regulation of TPX2 protein levels governs cell cycle progression in mouse oocytes. *PLoS ONE* **3**, e3338.

Chen, J., Melton, C., Suh, N., Oh, J. S., Horner, K., Xie, F., Sette, C., Blelloch, R. and Conti, M. (2011). Genome-wide analysis of translation reveals a critical role for deleted in azoospermia-like (Dazl) at the oocyte-to-zygote transition. *Genes Dev.* **25**, 755-766.

Chen, J., Torcia, S., Xie, F., Lin, C.-J., Cakmak, H., Franciosi, F., Horner, K., Onodera, C., Song, J. S., Cedars, M. I. et al. (2013). Somatic cells regulate maternal mRNA translation and developmental competence of mouse oocytes. *Nat. Cell Biol.* **15**, 1415-1423.

Eckerdt, F., Pascreau, G., Phistry, M., Lewellyn, A. L., DePaoli-Roach, A. A. and Maller, J. L. (2009). Phosphorylation of TPX2 by Plx1 enhances activation of Aurora A. *Cell Cycle* **8**, 2413-2419.

Fan, H.-Y. and Sun, Q.-Y. (2004). Involvement of mitogen-activated protein kinase cascade during oocyte maturation and fertilization in mammals. *Biol. Reprod.* **70**, 535-547.

Fan, H.-Y., Liu, Z., Shimada, M., Sterneck, E., Johnson, P. F., Hedrick, S. M. and Richards, J. S. (2009). MAPK3/1 (ERK1/2) in ovarian granulosa cells are essential for female fertility. *Science* **324**, 938-941.

Helmke, K. J. and Heald, R. (2014). TPX2 levels modulate meiotic spindle size and architecture in Xenopus egg extracts. *J. Cell Biol.* **206**, 385-393.

Ivshina, M., Lasko, P. and Richter, J. D. (2014). Cytoplasmic polyadenylation element binding proteins in development, health, and disease. *Annu. Rev. Cell Dev. Biol.* **30**, 393-415.

Keady, B. T., Kuo, P., Martinez, S. E., Yuan, L. and Hake, L. E. (2007). MAPK interacts with XGef and is required for CPEB activation during meiosis in Xenopus oocytes. *J. Cell Sci.* **120**, 1093-1103.

Komrskova, P., Susor, A., Malik, R., Prochazkova, B., Liskova, L., Supolikova, J., Hladky, S. and Kubelka, M. (2014). Aurora kinase A is not involved in CPEB1 phosphorylation and cyclin B1 mRNA polyadenylation during meiotic maturation of porcine oocytes. *PLoS ONE* **9**, e101222.

Lefebvre, C., Terret, M. E., Djiane, A., Rassinier, P., Maro, B. and Verlhac, M.-H. (2002). Meiotic spindle stability depends on MAPK-interacting and spindle-stabilizing protein (MISS), a new MAPK substrate. *J. Cell Biol.* **157**, 603-613.

Liu, Y., Lu, X., Shi, J., Yu, X., Zhang, X., Zhu, K., Yi, Z., Duan, E. and Li, L. (2016). BTG4 is a key regulator for maternal mRNA clearance during mouse early embryogenesis. *J. Mol. Cell Biol.* **8**, 366-368.

Martinez, S. E., Yuan, L., Lacza, C., Ransom, H., Mahon, G. M., Whitehead, I. P. and Hake, L. E. (2005). XGef mediates early CPEB phosphorylation during Xenopus oocyte meiotic maturation. *Mol. Biol. Cell* **16**, 1152-1164.

Mendez, R., Barnard, D. and Richter, J. D. (2002). Differential mRNA translation and meiotic progression require Cdc2-mediated CPEB destruction. *EMBO J.* **21**, 1833-1844.

Moore, G. D., Ayabe, T., Kopf, G. S. and Schultz, R. M. (1996). Temporal patterns of gene expression of G1-S cyclins and cdks during the first and second mitotic cell cycles in mouse embryos. *Mol. Reprod. Dev.* **45**, 264-275.

Piccioni, F., Zappavigna, V. and Verrotti, A. C. (2005). Translational regulation during oogenesis and early development: the cap-poly(A) tail relationship. *C. R. Biol.* **328**, 863-881.

Pique, M., Lopez, J. M., Foissac, S., Guigo, R. and Mendez, R. (2008). A combinatorial code for CPE-mediated translational control. *Cell* **132**, 434-448.

Reverte, C. G., Ahearn, M. D. and Hake, L. E. (2001). CPEB degradation during Xenopus oocyte maturation requires a PEST domain and the 26S proteasome. *Dev. Biol.* **231**, 447-458.

Setoyama, D., Yamashita, M. and Sagata, N. (2007). Mechanism of degradation of CPEB during Xenopus oocyte maturation. *Proc. Natl. Acad. Sci. USA* **104**, 18001-18006.

Sousa Martins, J. P., Liu, X., Oke, A., Arora, R., Franciosi, F., Viville, S., Laird, D. J., Fung, J. C. and Conti, M. (2016). DAZL and CPEB1 regulate mRNA translation synergistically during oocyte maturation. *J. Cell Sci.* **129**, 1271-1282.

Development (2017) 144, 452-463 doi:10.1242/dev.144410

Su, Y.-Q., Sugiura, K., Woo, Y., Wigglesworth, K., Kamdar, S., Affourtit, J. and Eppig, J. J. (2007). Selective degradation of transcripts during meiotic maturation of mouse oocytes. *Dev. Biol.* **302**, 104-117.

Terret, M. E., Lefebvre, C., Djiane, A., Rassinier, P., Moreau, J., Maro, B. and Verlhac, M.-H. (2003). DOC1R: a MAP kinase substrate that control microtubule organization of metaphase II mouse oocytes. *Development* **130**, 5169-5177.

Verlhac, M. H., Kubiak, J. Z., Weber, M., Geraud, G., Colledge, W. H., Evans, M. J. and Maro, B. (1996). Mos is required for MAP kinase activation and is involved in microtubule organization during meiotic maturation in the mouse. *Development* **122**, 815-822.

Yu, C., Ji, S.-Y., Dang, Y.-J., Sha, Q.-Q., Yuan, Y.-F., Zhou, J.-J., Yan, L.-Y., Qiao, J., Tang, F. and Fan, H.-Y. (2016a). Oocyte-expressed yes-associated protein is a key activator of the early zygotic genome in mouse. *Cell Res.* **26**, 275-287.

Yu, C., Ji, S.-Y., Sha, Q.-Q., Dang, Y., Zhou, J.-J., Zhang, Y.-L., Liu, Y., Wang, Z.-W., Hu, B., Sun, Q.-Y. et al. (2016b). BTG4 is a meiotic cell cycle-coupled maternal-zygotic-transition licensing factor in oocytes. *Nat. Struct. Mol. Biol.* **23**, 387-394.

Zhang, Y.-L., Liu, X.-M., Ji, S.-Y., Sha, Q.-Q., Zhang, J. and Fan, H.-Y. (2015). ERK1/2 activities are dispensable for oocyte growth but are required for meiotic maturation and pronuclear formation in mouse. *J. Genet. Genomics* **42**, 477-485.

Supplementary Table 1.Antibody information.

Protein name	Manufacture (catalogue number)	Applications (working dilution)
FITC-α-Tubulin	Sigma (F2168)	IF (1:500)
CNOT7	Santa Cruz (sc-101009)	WB (1:200)
ERK1/2	Santa Cruz (sc-94)	WB (1:1000)
p-ERK1/2	Cell Signaling (9101S)	IF (1:400)
HA	Cell Signalling (3724)	WB (1:2000)
FLAG	Sigma (F3165)	WB (1:3000)
BTG4	Abcam (ab206914)	WB (1:500)
CPEB1	Proteintech(13274-1-AP)	WB (1:500)
TPX2	Novus Biologicals(NB500-183)	WB (1:2000)，IF (1:1000)
CyclinB	Cell Signaling (4138)	WB (1:500)
MYC	Cell Signaling (2272)	WB (1:1000)
CREST	Fitzgerald Industries International (70R-21494)	IF (1:100)
TOP2B	Abcam (ab109524)	IF (1:200)
DDB1	Epitomics (3821-1)	WB (1:10000)
WEE2	Proteintech(55119-1-AP)	WB (1:500)

Supplementary Table 2. Primer sequences.

Primer name	Genes targeted	Application	Sequences (5'-3')
Cre-1	*Gdf9-Cre*	Genotyping (420bp)	5'-AAGAACCTGATGGACATGTTCAG-3'
Cre -2			5'-CTGATTCTGGCAATTTCGG-3'
P1	N.A.	Anchor primer (C10T2) and PAT2 for PAT assay	5'- CCCCCCCCCCTT -3'
P2			5'-CAGGAAACAGCTATGACCCCCCCCCCTT-3'
Ccnb1-F	*Ccnb1*	PAT assay (with P2)	5'-CCACTCCTGTCTTGTAATGC-3'
Dazl-F	*Dazl*	PAT assay (with P2)	5'-GAGAAGGGAGAAAGAGACAAG-3'
Tex19.1-F	*Tex19.1*	PAT assay (with P2)	5'-TCTGGCATGTTCGTGTCAGTG-3'
Bub1b-F	*Bub1b*	PAT assay (with P2)	5'-CTGGTCTGGGGCTGCTGTGAT-3'
Tpx2-F	*Tpx2*	PAT assay (with P2)	5'-GGTGTGGCCTGGTTGGAGTAG-3'
Rps2-F	*Rps2*	Real-time PCR (165bp)	5'-GCCACCTTTGATGCCATCT-3'
Rps2-R			5'-TGTGGTAGCCACAGCTGGA-3'
Fgf8-F	*Fgf8*	Real-time PCR (180bp)	5'-CTTTTGGAAGCAGAGTCCGA-3'
Fgf8-R			5'-CCATGTACCAGCCCTCGTAC-3'
Zp2-F	*Zp2*	Real-time PCR (161bp)	5'-GCAGCTGGAGCTCTTGTTCT-3'
Zp2-R			5'-TCCATTGTCCAAAGTCCACA-3'
Tceb1-F	*Tceb1*	Real-time PCR (176bp)	5'-ATCTTCTGATGGCCATGAATTT-3'
Tceb1-R			5'-CCTTGTAGGTAAAATACATGCACAC-3'
Padi6-F	*Padi6*	Real-time PCR (231bp)	5'-AGTGTATCAGCCTGAACCGC-3'
Padi6-R			5'-AGGTGCCATTGATTTTGGG-3'

Nobox-F	*Nobox*	Real-time PCR (153bp)	5’-CATGAAGGGGACCTGAAGAA-3’
Nobox-R			5’-GGAAATCTCATGGCGTTTGT-3’
Paip2-F	*Paip2*	Real-time PCR (200bp)	5’-AGAGCGCCTATGTGTGGTGT-3’
Paip2-R			5’-TCTCCCACACAAGTCTTGCC-3’
Polr2d-F	*Polr2d*	Real-time PCR (164bp)	5’-AGTTTGAGTTGGCCTGTTTAGC-3’
Polr2d-R			5’-AGTGACGTCTGCGGATCAGT-3’